Sub-barrier fusion of ^{37}Cl+ ^{70,72,73,74,76}Ge

E. Martínez-Quiroz and E. F. Aguilera

Instituto Nacional de Investigaciones Nucleares, Departamento del Acelerador, Apartado Postal 18-1027, Código Postal 11801, México, Distrito Federal, México

J. J. Kolata and M. Zahar

Physics Department, University of Notre Dame, Notre Dame, Indiana 46556

Fusion excitation functions were obtained for ^{37}Cl+ ^{70,72,73,74,76}Ge at energies from about 6 MeV below to 7 MeV above the Coulomb barrier. The barrier parameters extracted from the data agree within 3% with those obtained from the systematics for fusion above the barrier. Low-energy enhancements are observed, whose behavior is explained within the context of simple model calculations by assigning appropriate degrees of freedom to the respective reaction partners. These degrees of freedom reflect the shape transition between spherical ^{70,72,73}Ge and prolate-deformed ^{74,76}Ge, and show also remarkable effects of the odd-A structure of ^{73}Ge. The results are consistent with those of similar analysis of different data sets where the same targets were used. The possible effects of double identical-phonon states for spherical nuclei, hexadecapole deformations for deformed ones, and nucleon transfer are also examined. An analysis of the barrier distributions is made, which indicates consistency with the assumed degrees of freedom.

PACS number(s): 25.70.Jj

I. INTRODUCTION

It has been well recognized that the fusion cross sections of heavy ions at energies near and below the Coulomb barrier might be strongly influenced by the coupling of intrinsic degrees of freedom of the target and/or the projectile to the corresponding relative motion [1,2]. These degrees of freedom may provide favored channels to fusion and this can explain the enhanced cross sections observed for many systems with respect to the predictions of conventional barrier penetration models (BPMs), which successfully describe fusion above the Coulomb barrier by assuming a tunneling through a one-dimensional potential barrier. Different degrees of freedom have been considered in this context [1,2] among which are surface vibrations, static deformation, particle transfer, neck formation, etc., and much work has been dedicated to trying to find out which of these are the most relevant ones for given particular systems.

In previous works [3,4], we have measured and analyzed the fusion of two series of medium mass systems with common targets, and we have been able to fit them within a consistent physical scheme where the effects of either the static deformation or the collective vibrations of the target and/or the projectile, are enough to get a good description of the data. The fusion with the ^{70,72,73,74,76}Ge isotopes was measured for either ^{27}Al [3] or ^{16}O [4], and the results were consistent with a shape transition observed in other independent works [5–8], from spherical (or possibly oblate) shapes for ^{70,72,73}Ge to prolate-deformed shapes for ^{74,76}Ge. Spectroscopic information from the literature was used in all model calculations with only one free parameter, the depth of the nuclear ion-ion potential. The observed sub-barrier fusion enhancement was larger for the heavier projectile, consistent with the expectation that this enhancement should scale with the height of the Coulomb barrier [9]. According to this, the fusion of the same targets with an even heavier projectile should show an increased sensitivity to the internal degrees of freedom and therefore the shape transition effects should be more evident in this case. In this work we measured the ^{37}Cl+ ^{70,72,73,74,76}Ge systems, for which Z_pZ_t is 544, considerably larger than 416, the value corresponding to the Al+Ge systems. The main purpose was to investigate whether the same degrees of freedom, determined independently for Ge in the mentioned works, are suitable to properly describe the new Cl+Ge systems.

In the next section, the experimental procedure is described and the obtained excitation functions are presented. In Sec. III, a search is made of those model assumptions dealing with the shape of the reactant nuclei that better describe the excitation functions. Additional effects not accounted for in these models are discussed in Sec. IV and the experimental barrier distributions are extracted and analyzed in Sec. V. Finally, in Sec. VI, a summary and the conclusions of this work are presented.

II. EXPERIMENTAL METHOD AND RESULTS

The experiments were carried out using ^{37}Cl beams from the tandem FN Van de Graaff accelerator at the University of Notre Dame, with energies ranging from 94.5 to 116.5 MeV, in steps of 2 MeV. The targets, prepared by the vacuum evaporation technique, are as specified in Table I.

The major difficulty in detecting the evaporation residues (ER) from fusion comes from the fact that their angular distribution is always forward peaked, so that they are normally embedded in a large background arising from slit scattering and other similar types of events. It is thus necessary to reduce the intensity of the transmitted beam to a manageable counting rate and to identify the ER, separating them out from the residual beamlike particles that still reach the detection system. These objectives were achieved by means of an electrostatic deflector operating in combination with a

TABLE I. Characteristics of the targets used in this work. All targets were made with GeO_2 and their thicknesses were determined by energy-loss measurements of α particles from a ^{228}Th source.

Target	Thickness ($\mu g/cm^2$)	Carbon backing ($\mu g/cm^2$)	Isotopic composition (% of ^{70,72,73,74,76}Ge)
^{70}Ge	250(8)	20	96.75, 1.12, 0.29, 1.36, 0.48
^{72}Ge	144(5)	43	1.04, 96.23, 0.77, 1.63, 0.33
^{73}Ge	109(11)	40	0.86, 2.09, 94.50, 2.24, 0.31
^{74}Ge	125(4)	20	1.71, 2.21, 0.90, 94.48, 0.70
^{76}Ge	143(10)	20	7.69, 6.65, 1.69, 10.08, 73.89

time-of-flight/energy telescope (see Fig. 1). The fact that the beam and ER have, in general, different electrostatic rigidities allows one to separate them out by the transverse electric field produced in the deflector. The measurement of time and energy, on the other hand, allows for mass identification. Further details of the spectrometer can be found in Ref. [10]. The transmission efficiency of the ER through the spectrometer was determined empirically by elastic scattering of ions of similar atomic and mass numbers. To accomplish this, we measured the Rutherford scattering of ^{103}Rh ions on ^{60}Ni at a laboratory angle of 9.75° and at bombarding energies of 36, 39, and 42 MeV. No measurable mass dependence of the transmission was noted when a ^{81}Br beam was used at 42 and 45 MeV. By averaging the results of all five measurements, which did not show an appreciable energy variation, the experimental value of the transmission efficiency was determined to be $T = 0.780 \pm 0.045$ in the energy and mass ranges of interest. A Monte Carlo model that simulated the performance of the spectrometer gave results consistent with this value.

A system of four silicon surface barrier (SSB) detectors placed symmetrically at an angle of 15° with respect to the nominal beam direction was used to normalize the data. In the usual method, where only one monitor is used (or the less usual one with two monitors), the fast variation of the Rutherford cross section at small angles makes the results strongly dependent on equipment-alignment and beam-focusing conditions. There are five parameters that must be simultaneously determined, in principle, in order to eliminate this dependence. These are related to the beam direction (θ, ϕ), the beam spot position on target (x, y), and the normalizing factor given by the product of the integrated charge times the target thickness (Qt). It can be shown [11], how-

ever, that three detectors suffice to deduce Qt with high precision provided the beam inclination is not too great ($\leqslant 4°$). By using four monitors, a very reliable estimation of the associated uncertainty can be additionally obtained. A typical precision of about 1% in the normalization factors for the differential cross sections has been obtained with our method, which is about 20 (4) times better than that of the one- (two-) monitor method under reasonably good alignment conditions. A detailed description of our normalization method can be found in Ref. [11].

A set of angular distributions typical of each system is presented in Fig. 2. Since these distributions are symmetric around $\theta = 0°$, the measurement of positive and negative angles allows for interpolation to the important region of small angles, while determining at the same time the zero-degree position of the time-of-flight arm with high precision. The results of Gaussian fits to the data are shown as continuous curves in Fig. 2, with the corresponding widths indicated in the caption. Since particle evaporation is the dominant decay mode for compound nuclei in the present mass and energy range, the complete fusion cross sections were simply taken as the ER cross sections. We measured single-angle excitation functions at an angle of 2° or 3°. Integration of the Gaussian distributions of Fig. 2 over the whole solid angle gave total fusion cross sections for the selected energies, which were then used to scale the single-angle excitation functions. As the shape of these angular distributions does not change appreciably within the energy range covered by our experiments, this procedure is well justified.

Impurities in the isotopic composition of the targets and energy loss in them were accounted for as described in Ref. [3]. The resulting fusion cross sections are listed in Table II. The reported errors include the 2% uncertainty in the absolute normalization factors as well as the statistical errors. In
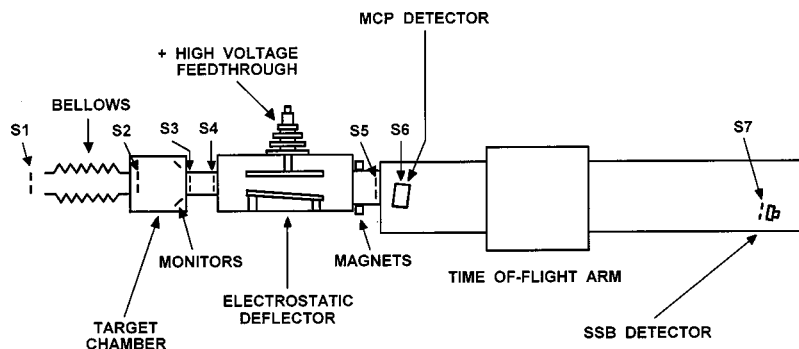

FIG. 1. Schematic side view of the spectrometer. $S1, \ldots, S7$ are slits whose positions and dimensions are important for the Monte Carlo calculations referred to in the text.
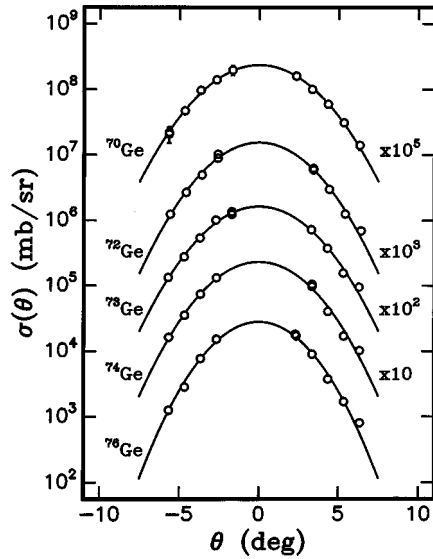
FIG. 2. Angular distributions of evaporation residues for ^{37}Cl + ^{70,72,73,74,76}Ge at $E_{c.m.}$=67.5, 72.4, 74.2, 74.5, and 75.1 MeV, respectively. Error bars smaller than the circles are not drawn. The standard deviations of the fitted Gaussians (solid lines) are 2.6°, 2.5°, 2.5°, 2.4°, and 2.2°, respectively.

addition, a maximum systematic error of about 7% is estimated for our data coming mainly from the transmission efficiency determination (~6%), the scaling of single-angle excitation functions (~2%), and the observation-angle error of the spectrometer (~2%). Since the corrections for isotopic impurities were very small for most data points, we neglected the corresponding contribution to the systematic error. The data are displayed in Fig. 3 for all systems, together with model calculations that will be discussed in the following sections.

III. BASIC ANALYSIS OF STATIC DEFORMATIONS AND COLLECTIVE VIBRATIONS

In order to study the possible effects of static deformations or surface vibrations of the target and/or the projectile on their corresponding fusion, the simplified coupled-channels code CCDEF [12] was used in the way described in Ref. [4]. Briefly, each reactant is assumed to be either spherical (S), oblate deformed (O), or prolate deformed (P), and the nucleus-nucleus potential depth is varied until the best fit to the experimental excitation function is achieved. Spherical nuclei are treated as vibrational while for statically deformed nuclei the sudden approximation is applied without explicitly including any excited state of the reactant. The several combinations of model assumptions for target-projectile systems (SS, SO, OP, etc.) produce, in general, different shapes for the excitation functions and the idea is to determine which combination, if any, gives a good description of the data. The resulting fusion barrier (obtained from the respective uncoupled calculation) is then tested by comparing it with the existing systematics from the BPM for fusion above the barrier.

As in previous works, our approach was to obtain all the

relevant nuclear structure information from the literature. The corresponding deformation parameters used in the code for the calculation of vibrational degrees of freedom are listed in Table III; for the case of ^{70,72,73,74,76}Ge, they are exactly the same ones used in Refs. [3,4]. For calculations where a static deformation was used, on the other hand, the deformation parameter for ^{37}Cl ($\beta_2=-0.18$) was calculated from the intrinsic electric quadrupole moment [13,14] and, for the case of ^{70,72,73,74,76}Ge, from the value of $|\beta_2|$ listed in Table III for the corresponding lowest transition, a procedure that can be justified within the adiabatic rotational model under the assumption of an axially symmetric nucleus, as noticed in Refs. [3,4] [note that in this case the sign of β is undetermined because of its square-root relation with $B(E2)$]. Although for the case of ^{37}Cl the shape (prolate or oblate) is specified by the sign of the intrinsic quadrupole moment (with negative sign corresponding to oblate deformation), it was decided to carry out the coupled-channels calculations for both shapes, fixing the magnitude of β_2 to the one given above, in order to test the sensitivity of sub-barrier fusion to the character of the deformation.

The values of χ^2 per degree of freedom obtained for each system under all nine model assumptions are presented in Table IV. It is clear from the table that the models OS, OO, PS, and PO can be immediately ruled out since the corresponding values of χ^2 are too large for all systems. If we restrict ourselves to the ^{37}Cl+^{70,72,73}Ge systems, on the other hand, we can also rule out all other models where ^{37}Cl is assumed to be either oblate or prolate deformed. Actually, picking the minimum value of χ^2 for each system would give the model sequence SS, SO, SS, SP, and SP for ^{37}Cl+^{70}Ge, ^{37}Cl+^{72}Ge, ^{37}Cl+^{73}Ge, ^{37}Cl+^{74}Ge, and ^{37}Cl+^{76}Ge, respectively.

This is consistent with the conclusions obtained with respect to the Ge isotopes in Ref. [3] from the Al+Ge systems, and in Ref. [4] from the O+Ge systems, i.e., the data favor either a spherical or an oblate-deformed model for ^{70,72}Ge (the results of these two models are nearly equivalent for these isotopes), while ^{73}Ge must be definitely spherical and for ^{74,76}Ge a prolate-deformed model is favored. The corresponding theoretical curves are plotted in Fig. 3 along with those of the related uncoupled calculations. A careful observation of the enhancements with respect to the uncoupled results indicates a qualitative change between ^{70,72}Ge and ^{73,74,76}Ge whereby the last three systems show a considerably larger enhancement, a feature that was also observed for the Al+Ge systems in Ref. [3] and, to a somewhat lesser extent, for the O+Ge systems in Ref. [4], but which appears much more conspicuous for these heavier systems. The enhancement factors plotted in Fig. 4 versus the center of mass energy relative to the respective fusion barriers, make this feature even more evident, and it strongly supports the conclusions of Refs. [3,4] about a structural change between ^{70,72}Ge and ^{73,74,76}Ge. This change is interpreted in the case of ^{73}Ge as due to the larger number of low-lying collective inelastic channels that can be coupled to the ground state with appreciable strength because of its odd-A nature (see Table III), and in the case of ^{74,76}Ge as a consequence of the mentioned transition from spherical (or possibly oblate)

TABLE II. Total fusion cross sections for ^{37}Cl+ ^{70,72,73,74,76}Ge.

System	$E_{c.m.}$ (MeV)	σ_{fus} (mb)	System	$E_{c.m.}$ (MeV)	σ_{fus} (mb)
^{37}Cl+ ^{70}Ge	62.47	0.065(31)		68.90	59.8(34)
	63.78	0.51(14)		70.23	87.3(49)
	65.07	3.67(28)		71.56	121.1(54)
	66.33	13.25(88)		72.89	156.7(72)
	67.54	31.4(22)		74.22	204.0(66)
	67.54	35.2(24)		75.21	238.(21)
	68.76	59.8(39)		76.87	292.(16)
	70.01	88.7(52)			
	71.29	120.8(71)	^{37}Cl+ ^{74}Ge	63.82	2.36(39)
	72.60	165.3(69)		65.15	6.82(73)
	73.90	205.4(93)		66.49	18.2(18)
	75.20	249.9(86)		67.83	43.4(29)
				69.16	70.9(40)
^{37}Cl+ ^{72}Ge	63.29	0.201(34)		70.50	108.7(57)
	64.60	1.72(37)		71.83	163.4(83)
	64.60	1.72(16)		73.16	204.(12)
	65.90	9.33(76)		74.50	265.(13)
	67.18	30.4(17)			
	68.46	58.6(25)	^{37}Cl+ ^{76}Ge	62.98	0.506(40)
	68.46	57.8(25)		64.33	3.26(44)
	69.76	93.4(40)		64.33	3.24(31)
	71.07	131.7(49)		64.33	3.19(18)
	72.39	190.(10)		65.67	12.4(11)
	72.39	180.3(76)		67.02	28.6(21)
	73.72	234.9(81)		68.38	48.5(30)
	75.03	281.(11)		69.72	82.7(51)
	76.35	310.(11)		71.06	138.0(77)
				72.41	190.1(90)
^{37}Cl+ ^{73}Ge	63.58	1.94(31)		73.41	250.(11)
	64.91	5.52(47)		75.09	287.(19)
	66.24	16.22(97)		75.09	288.(17)
	66.24	16.9(11)		75.09	296.(15)
	67.58	36.1(21)			

shapes for ^{70,72}Ge to prolate deformed shapes for ^{74,76}Ge. As for the ^{37}Cl projectile, the data for all systems analyzed in the present work are consistent, within the simple scheme used so far, with the results of using a spherical (vibrational) model for this nucleus. Even though this might seem reasonable if we consider the semimagical nature of ^{37}Cl, this nucleus has a negative intrinsic quadrupole moment, as mentioned above, which indicates a (moderate) oblate deformation. In fact, a previous analysis of sub-barrier fusion for some Cl+Ni systems [15] clearly favored an oblate model for ^{37}Cl. In the next section we will investigate the possibility of using an oblate-deformed model for ^{37}Cl, but adding different effects not included in the previous scheme.

IV. MULTIPHONONS, HEXADECAPOLE DEFORMATIONS, AND NUCLEON TRANSFER

The model calculations described in the previous section are generally limited in several aspects. We will now discuss

some of these limitations and their possible influence on the conclusions. The possible effects of the coupling of two-phonon states in vibrational nuclei on fusion processes have been studied by several authors [16–20] and its importance has been well established for several systems. Some evidence has been found for the two-phonon structure of the 0_2^+, 2_2^+, and 4_1^+ states in ^{70,72}Ge from proton [21,22], deuteron [23], and Li [22] scattering studies. One may thus ask about the possible effects of such states on the fusion of these nuclei with ^{37}Cl. It would be interesting to know, for example, if a model OS that includes double identical-phonon states for the target could properly describe the experimental excitation functions for ^{37}Cl+ ^{70,72}Ge, which could certainly change our previous conclusions. Although CCDEF is able to take account of multiple-phonon excitations, including, e.g., two-phonon states formed by mutual excitation, those in which the same phonon is doubly excited cannot be handled with this code [2,18].

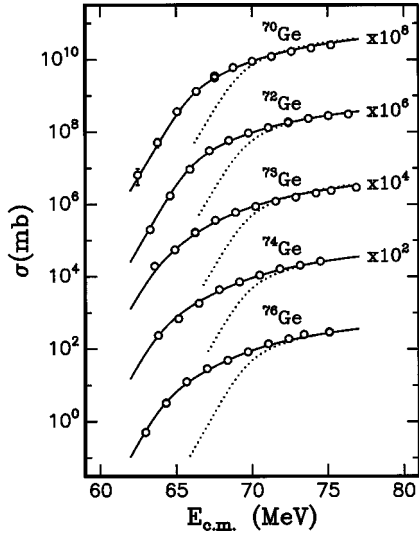In order to estimate the possible effect of double

FIG. 3. Experimental fusion cross sections and SS, SO, SS, SP, and SP models (solid lines) for ^{37}Cl+ ^{70}Ge, ^{37}Cl+ ^{72}Ge, ^{37}Cl + ^{73}Ge, ^{37}Cl+ ^{74}Ge, and ^{37}Cl+ ^{76}Ge, respectively. These curves are undistinguishable from the transfer calculations of Sec. IV. The dotted lines correspond to one-dimensional barrier penetration calculations.

identical-phonon excitations in ^{70,72}Ge, we first assumed an OS model and the oblate-deformed nature of ^{37}Cl was treated as in CCDEF. In regard to the target, we used the method of Kruppa *et al.* [18] to include the double-phonon

TABLE III. Inelastic channels included in the coupled-channel calculations and respective coupling parameters.

Nucleus	J^π	E_x (MeV)	λ	β_λ
^{37}Cl	$\frac{1}{2}^+$	1.73	2	0.14
	$\frac{5}{2}^+$	3.09	2	0.24
	$\frac{7}{2}^-$	3.10	3	0.32
	$\frac{9}{2}^-$	4.01	3	0.33
^{70}Ge	2^+	1.04	2	0.23
	3^-	2.56	3	0.23
^{72}Ge	2^+	0.83	2	0.25
	3^-	2.51	3	0.24
^{73}Ge	$\frac{5}{2}^+$	0.013	2	0.24
	$\frac{7}{2}^+$	0.069	2	0.32
	$\frac{7}{2}^+$	0.499	2	0.13
	$\frac{13}{2}^+$	0.826	2	0.27
^{74}Ge	2^+	0.60	2	0.29
	3^-	2.54	3	0.16
^{76}Ge	2^+	0.56	2	0.27
	3^-	2.69	3	0.14

states. We assumed that the 2^+ state and the 3^- state shown in Table III for ^{70,72}Ge behave like a quadrupole and octupole phonon, respectively, as was in fact assumed in all those model calculations of Table IV in which a spherical target was assumed. In CCDEF the basis states included are the ground state 0^+, the two one-phonon states 2^+ and 3^-, and the product two-phonon state $2^+ \otimes 3^-$. The corresponding inelastic channels are treated as independent modes that couple to the initial ground state. The coupling interaction is thus reduced to a 4×4 matrix, which is diagonalized at the barrier (constant coupling approximation) to yield the eigenchannels [18,24].

The idea now is to include, in addition to the CCDEF basis states mentioned above, the other two types of two-phonon states, $(2^+)^2$ and $(3^-)^2$, corresponding to two quadrupole and two octupole phonons, which it can be shown [18], results in a 6×6 coupling matrix that can be numerically diagonalized. As before, the depth of the nuclear ion-ion potential was varied until the best fit to the data was achieved. This procedure gave χ^2 values of 16.3 and 5.7 for ^{70,72}Ge, respectively. For the case of ^{73}Ge there is no good evidence, to our knowledge, for the existence of double-phonon states, although this possibility seems to be consistent with the results of a Coulomb excitation study [25]. For completeness, we did also the OS calculations with double identical-phonons for this system. The four double-phonon states corresponding to the single-phonon states of Table III were added to the 16 basis states used by CCDEF in this case, leading to a 20×20 matrix. Repeating the procedure for this new matrix gave $\chi^2 = 8.2$ for this case. Even though the fits of the OS models to the data were certainly improved by the inclusion of double identical-phonon states in the previous calculations for the three analyzed systems, the corresponding SS models still give a better description of the data, as can be seen from Table IV. It remains to estimate the effects of double phonons in Ge upon these SS models. Since we now have to include the four excited states in the projectile, the basis space becomes much larger. Keeping only up to two-phonon states in ^{37}Cl and ^{70,72}Ge, with double identical-phonons in ^{70,72}Ge but not in ^{37}Cl, we get a 66×66 coupling matrix. Upon diagonalization, we get best fits with χ^2 values of 3.0 and 3.9 for ^{70,72}Ge, respectively. A comparison with the values obtained for the corresponding SS models in Table IV indicates negligible effects of double identical-phonons for these cases. A similar result is expected for ^{73}Ge, but the explicit calculation was not done since the corresponding coupling matrix would be far too large (165 $\times$ 165) for this case. We conclude, therefore, that the inclusion of double identical-phonon states in the analysis could not possibly change our previous conclusions about the data favoring a spherical projectile and, in fact, their effect on the SS models is negligible.

All our calculations referring to a deformed target in the previous section included only quadrupole deformations. For some systems such as ^{16}O+ ^{154}Sm [26,27] and ^{16}O+ ^{186}W [28], the data show a strong sensitivity of fusion to the hexadecapole deformation. In order to test for possible effects of higher-order deformations in our systems, a hexadecapole deformation was added for ^{74,76}Ge with β_4 values of 0.022

TABLE IV. Value of χ^2 for the different model predictions for each system. O, P, and S in the first (second) place implies Cl(Ge) oblate, prolate, and spherical, respectively.

System	Model								
	OO	OP	OS	PO	PP	PS	SO	SP	SS
^{37}Cl+ ^{70}Ge	30.7	16.9	19.9	25.3	14.8	15.7	4.8	3.5	3.3
^{37}Cl+ ^{72}Ge	15.2	9.3	6.4	11.5	12.9	5.0	1.5	19.9	3.7
^{37}Cl+ ^{73}Ge	60.1	38.1	8.9	53.1	34.5	7.5	20.8	10.7	4.1
^{37}Cl+ ^{74}Ge	12.9	2.4	9.5	10.2	1.7	7.1	3.0	1.5	3.1
^{37}Cl+ ^{76}Ge	33.7	4.2	26.7	22.6	2.4	16.6	8.3	2.2	8.5

[29] and 0.02 [30], respectively, and a CCDEF fit was made to the data using the SP model. The corresponding results show that the hexadecapole deformations in ^{74,76}Ge produce only a small effect, so that our previous conclusions about the SP model giving a good description of the data for the ^{37}Cl + ^{74,76}Ge systems remain valid.

The coupling form factors used here make use of the conventional linear coupling approximation, where the coupling potential is expanded in powers of the deformation parameter, keeping only the linear term. It was shown recently [31] that higher order couplings to nuclear surface vibrations might produce dramatic effects especially in the fusion of nearly symmetric systems with large values of $Z_p Z_t$, above 1000. For our systems this product is 544, a value rather similar to that of the ^{16}O+ ^{144}Sm system, which was also analyzed in Ref. [31], showing only small effects of higher order couplings, especially as far as the excitation function is concerned. Since the deformation parameters in Ge are also similar to those in Sm, we might expect similar coupling strengths in our systems and in O+Sm, and therefore similar effects in our systems to those calculated for this last system. We thus conclude that no significant effects are expected in our theoretical excitation functions for Cl+Ge upon inclusion of higher order couplings in the calculations.

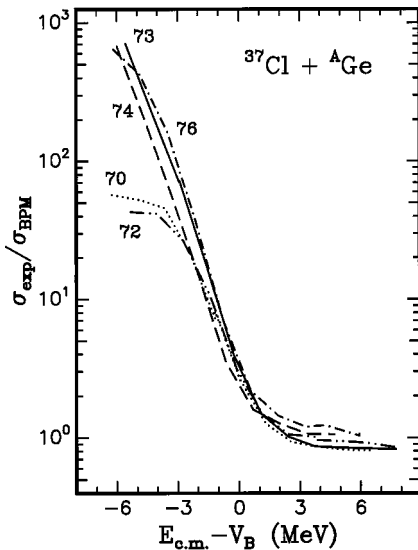It has been suggested [32] that fusion will be favored in a

transfer channel if Q_{eff} is positive, where Q_{eff} is the sum of the ground state Q value and the difference between the Coulomb barriers of the entrance and exit channels. With the aim of obtaining an estimate of the relative importances of one-nucleon transfer channels, a CCDEF calculation was performed assuming an oblate-deformed ^{37}Cl and using for each system that channel with the largest Q_{eff} value, which is the one-proton pickup channel for ^{37}Cl+ ^{70}Ge and the one-proton stripping channel for all the other systems. Actually, it is also true that no two-nucleon transfer channel has a larger Q_{eff} value than these channels. Only transfer to ground states was considered and both, the depth of the nuclear potential and the strength F_{tr} of the transfer coupling were simultaneously varied to get the best fit to the data. A spherical (prolate-deformed) model was assumed for ^{70,72,73}Ge (^{74,76}Ge) in these calculations. Except for the ^{37}Cl+ ^{70}Ge system, smaller or similar χ^2 values were obtained (χ^2=1.9,0.6,0.8,1.2 and F_{tr}=2.1,3.5,1.5,1.0 for ^{37}Cl+ ^{72,73,74,76}Ge, respectively) as those corresponding to the best fit of Table IV. Even for the ^{37}Cl+ ^{70}Ge system, the results (χ^2=6.1, F_{tr}=1.6) are not too discouraging. When we include, for example, the one-proton stripping channel in addition to the one previously considered for this system, we obtain χ^2=2.3 with F_{tr}=0.6 (3.0) for pickup (stripping). Using this last result for this system and the ones previously mentioned for ^{72,73,74,76}Ge, the corresponding theoretical curves are undistinguishable from those of the spherical Cl models plotted in Fig. 3. The transfer strengths obtained in this phenomenological approach have similar values to those used in Ref. [33] for Si+Ni systems. Although more accurate coupled-channel calculations are needed, it seems quite feasible that one-nucleon transfer between an oblate-deformed ^{37}Cl and the (vibrational or prolate-deformed) Ge targets might well be the underlying mechanism that accounts for the observed sub-barrier fusion enhancements.

V. ONE-DIMENSIONAL BARRIERS AND BARRIER DISTRIBUTIONS

By using the potential depths obtained from the fits of the best spherical Cl models and those of the oblate-deformed Cl models plus transfer, the fusion barrier parameters were calculated for all systems. The resulting radius R_0, height V_0, and curvature parameter $\hbar\omega_0$ are tabulated in Table V, along with the systematics reported in Refs. [34,35]. We see that, for the case of the spherical Cl models, the extracted barriers

FIG. 4. Enhancement factors for ^{37}Cl+ ^{70,72,73,74,76}Ge as a function of the energy excess with respect to the barrier.

TABLE V. Barrier parameters extracted from our data and from the systematics of Refs. [34,35]. For each system, the first line corresponds to the best spherical Cl model while the second line refers to the oblate Cl model plus transfer.

	This work			Ref. [34]		Ref. [35]	
System	R_0 (fm)	V_0 (MeV)	$\hbar\omega_0$ (MeV)	R_0 (fm)	V_0 (MeV)	R_0 (fm)	V_0 (MeV)
^{37}Cl+ ^{70}Ge	10.7	68.7	3.8	10.3	70.8	10.1	68.6
	10.6	69.4	3.8				
^{37}Cl+ ^{72}Ge	10.6	69.0	3.8	10.3	70.4	10.1	68.2
	10.7	68.8	3.8				
^{37}Cl+ ^{73}Ge	10.6	69.2	3.7	10.4	70.2	10.1	68.0
	10.4	70.2	3.7				
^{37}Cl+ ^{74}Ge	10.7	68.7	3.7	10.4	70.0	10.1	67.8
	10.6	69.0	3.7				
^{37}Cl+ ^{76}Ge	10.7	68.4	3.7	10.4	69.7	10.2	67.5
	10.7	68.7	3.7				

agree better (within less than 2%) with the values resulting from the formulas of Ref. [35], while for the oblate-Cl models no systematic behavior is observed. In all cases, the extracted barriers have a value above that from Ref. [35] and below that from Ref. [34]. The radii, on the other hand, always agree better (within less than 4%) with those obtained from Ref. [34]. From the discussions in both Refs. [34,35], the observed deviations between the extracted and calculated barriers seem to be reasonable in any case.

The distribution of fusion barriers can be deduced from the curvature $d^2(E\sigma)/dE^2$ of $E\sigma(E)$ [36]. Since the main purpose of this work could be achieved by having just the excitation functions, the experiments were not designed with the small energy steps and very high statistics required to have high quality barrier distributions, but these distributions are calculated here anyway as a consistency check. A three-point formula with variable step was used to numerically evaluate second derivatives for our data. In order to keep statistical uncertainties at a reasonably low value, a three-point average was first done to smooth out the excitation functions and most of the derivatives were calculated using second nearest neighbors, except for the lowest energy point for which it was necessary to use first nearest neighbors. Since the numerical derivatives may be quite sensitive to the step ΔE used to evaluate them, it is important to use the same ΔE for both the data and the theoretical predictions. We used $\Delta E = 1.3$ MeV to obtain the derivatives of the calculated cross sections in the region around the lowest energy data point, and $\Delta E = 2.6$ MeV for higher energies. The two curves thus obtained were then joined by straight lines, with the sizes of the regions chosen so as to obtain composite curves as smooth as possible, although this goal was not always completely achieved.

The results are presented in Fig. 5 for all measured systems, along with theoretical curves obtained by taking the numerical derivative of either the spherical Cl best models (solid lines) or the transfer models just discussed (dashed lines). The errors in the derivatives become too high at the higher energies, but the quality of the data was good enough to appreciate the good fits to the low energy points. The two

models corresponding to the solid and dashed curves for each system cannot be discriminated from these data. Summarizing, we could actually say that, within the error bars, this analysis of barrier distributions gives results consistent with the shape transition between ^{70,72,73}Ge and ^{74,76}Ge, but would accept either a vibrational Cl model or an oblate-deformed Cl model with nucleon transfer for all systems.

VI. SUMMARY AND CONCLUSIONS

The near and sub-barrier fusion cross sections for the ^{37}Cl+ ^{70,72,73,74,76}Ge systems have been measured using a time-of-flight spectrometer coupled to an electrostatic deflector. A structural change was apparent in the excitation func-
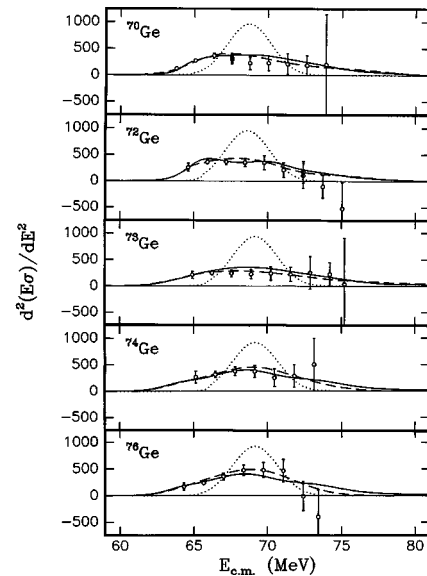

FIG. 5. Barrier distributions extracted from our data and theoretical predictions. Continuous lines correspond to the SS, SO, SS, SP, and SP model for ^{70}Ge, ^{72}Ge, ^{73}Ge, ^{74}Ge, and ^{76}Ge, respectively. Dashed lines refer to the models using an oblate-deformed Cl with nucleon transfer, as discussed in the text. The dotted lines correspond to the BPM for all cases.

tions between the two lightest and the three heaviest targets, whereby these last ones showed a much larger low-energy enhancement, with respect to the one-dimensional barrier penetration prediction. From all possible combinations involving the vibrational or statically deformed nature of the reactants, a consistent scheme was found that properly described all features of the data, including the barrier distributions. A vibrational character had to be assumed for the ^{70,72,73}Ge targets, while the heavier Ge isotopes had to be assumed to be prolate deformed. Consistent with previous results for fusion of ^{27}Al [3] and ^{16}O [4] with the same targets, the structural change in the excitation functions was thus associated with the shape transition between the spherical (or possibly oblate) ^{70,72}Ge isotopes and the prolate-deformed ^{74,76}Ge nuclei, and to the effect of the odd-*A* character for the case of ^{73}Ge, which provides more low-lying collective inelastic channels that can be coupled to the ground state with appreciable strength. It is important to note that the same degrees of freedom used for the Ge isotopes in Refs. [3,4] with the same coupling strengths were also used here. Shape transition effects have been searched for recently in sub-barrier fusion data of rare earth nuclei, where they were predicted to be noticeable by the different skewness of the barrier distributions for oblate and prolate nuclei [2]. In this work we corroborate our previous finding that, for the

Ge isotopes, the corresponding shape transition is quite obviously reflected in the excitation functions themselves, especially when they are plotted in the form of enhancement factors, as in Fig. 4. In addition, the nuclear structure effects related to the odd-*A* character in the case of ^{73}Ge are also remarkable in this kind of plot.

As for the projectile, the present data could not discriminate between the assumption of a spherical (vibrational) ^{37}Cl or an oblate-deformed ^{37}Cl with nucleon transfer, but this last assumption would be consistent with the results of a previous analysis of sub-barrier fusion data for Cl+Ni systems [15] in that an oblate model was necessary there for ^{37}Cl. Consideration of double-phonon states in ^{70,72,73}Ge and hexadecapole deformations in ^{74,76}Ge was shown to be unimportant. An argument was given as well to indicate that the inclusion of higher order couplings would also not change the conclusions.

ACKNOWLEDGMENTS

[1] M. Beckerman, Rep. Prog. Phys. **51**, 1047 (1988).

[2] A. B. Balantekin and N. Takigawa, Rev. Mod. Phys. **70**, 77 (1998).

[3] E. F. Aguilera, J. J. Vega, J. J. Kolata, A. Morsad, R. J. Tighe, and X. J. Kong, Phys. Rev. C **41**, 910 (1990).

[4] E. F. Aguilera, J. J. Kolata, and R. J. Tighe, Phys. Rev. C **52**, 3103 (1995).

[5] R. Lecomte, G. Kajrys, S. Landsberger, P. Paradis, and S. Monaro, Phys. Rev. C **25**, 2812 (1982).

[6] S. Sen, S. E. Darden, R. C. Luhn, N. O. Gaiser, G. Murillo, and J. Ramirez, Phys. Rev. C **31**, 787 (1985).

[7] F. Ballester, E. Casal, and J. B. A. England, Nucl. Phys. **A490**, 227 (1988).

[8] E. Landulfo, R. N. Saxena, C. B. Zamboni, and A. L. Lapolli, Phys. Rev. C **50**, 733 (1994).

[9] R. Lindsay and N. Rowley, J. Phys. G **10**, 805 (1984).

[10] E. F. Aguilera, J. J. Vega, and J. J. Kolata, Rev. Mex. Fis. **43**, 622 (1997).

[11] E. F. Aguilera, J. J. Vega, E. Martinez, J. J. Kolata, and A. Morsad, Rev. Mex. Fis. **35**, 489 (1989).

[12] J. Fernandez Niello, C. H. Dasso, and S. Landowne, Comput. Phys. Commun. **54**, 409 (1989).

[13] M. Eibel and R. Quad, Z. Naturforsch. Teil **41A**, 15 (1986).

[14] P. Raghavan, At. Data Nucl. Data Tables **42**, 189 (1989).

[15] J. J. Vega, E. F. Aguilera, G. Murillo, J. J. Kolata, A. Morsad, and X. J. Kong, Phys. Rev. C **42**, 947 (1990).

[16] N. Takigawa and T. Ikeda, in *Proceedings on the Many Facets of Heavy Ion Fusion Reactions*, edited by W. Henning *et al.* (Report No. ANL-PHY-86-1, Argonne National Laboratory, 1986), p. 613.

[17] H. Esbensen and S. Landowne, Phys. Rev. C **35**, 2090 (1987); Nucl. Phys. **A492**, 473 (1989).

[18] A. T. Kruppa, P. Romain, M. A. Nagarajan, and N. Rowley, Nucl. Phys. **A560**, 845 (1993).

[19] A. M. Stefanini, D. Ackermann, L. Corradi, D. R. Napoli, C. Petrache, P. Spolaore, P. Bednarczyk, H. Q. Zhang, S. Beghini, G. Montagnoli, L. Mueller, F. Scarlassara, G. F. Segato, F. Soramel, and N. Rowley, Phys. Rev. Lett. **74**, 864 (1995).

[20] A. M. Stefanini, D. Ackermann, L. Corradi, J. H. He, G. Montagnoli, S. Beghini, F. Scarlassara, and G. F. Segato, Phys. Rev. C **52**, R1727 (1995).

[21] T. H. Curtis, H. F. Lutz, and W. Bartolini, Phys. Rev. C **1**, 1418 (1970).

[22] J. Jabbour, L. H. Rosier, E. I. Obiajunwa, and B. Ramstein, Nucl. Phys. **A500**, 356 (1989).

[23] G. Szaloky, L. A. Montestruque, M. C. Cobian-Rozak, and S. E. Darden, Phys. Rev. C **18**, 750 (1978).

[24] C. H. Dasso, S. Landowne, and A. Winther, Nucl. Phys. **A407**, 221 (1983).

[25] G. C. Salzman, A. Goswami, and D. K. McDaniels, Nucl. Phys. **A192**, 312 (1972).

[26] J. R. Leigh, N. Rowley, R. C. Lemmon, D. J. Hinde, J. O. Newton, J. X. Wei, J. C. Mein, C. R. Morton, S. Kuyucak, and A. T. Kruppa, Phys. Rev. C **47**, R47 (1993).

[27] T. Izumoto, T. Udagawa, and B. T. Kim, Phys. Rev. C **51**, 761 (1995).

[28] R. C. Lemmon, J. R. Leigh, J. X. Wei, C. R. Morton, D. J. Hinde, J. O. Newton, J. C. Mein, N. Dasgupta, and N. Rowley, Phys. Lett. B **316**, 32 (1993).

[29] L. H. Rosier and E. I. Obiajunwa, Nucl. Phys. **A500**, 323 (1989).

[30] B. Ramstein, R. Tamisier, L. H. Rosier, and P. Avignon, Nucl. Phys. **A411**, 231 (1983).

[31] K. Hagino, N. Takigawa, M. Dasgupta, D. J. Hinde, and J. R. Leigh, Phys. Rev. C **55**, 276 (1997).

[32] R. A. Broglia, C. H. Dasso, S. Landowne, and A. Winther, Phys. Rev. C **27**, 2433 (1983).

[33] S. Landowne, S. C. Pieper, and F. Videbaek, Phys. Rev. C **35**, 597 (1987).

[34] L. C. Vaz, J. M. Alexander, and G. R. Satchler, Phys. Rep. **69**, 373 (1981).

[35] R. K. Puri and R. K. Gupta, in *Heavy-Ion Fusion: Exploring the Variety of Nuclear Properties*, Proceedings of the Workshop, Padova, Italy, 1994, edited by A. M. Stefanini, G. Nebbia, S. Lunardi, G. Montagnoli, and A. Vitturi (World Scientific, Singapore, 1994).

[36] N. Rowley, G. R. Satchler, and P. Stelson, Phys. Lett. B **254**, 25 (1991).